Geometrical control of dissipation in the spreading of fluids on soft solids

Supplementary Materials

Menghua Zhao,[1,2] Julien Dervaux,[1] Tetsuharu Narita,[2,3]
François Lequeux,[2] Laurent Limat,[1] and Matthieu Roché[1,*]

[1]*Matière et Systèmes Complexes, CNRS UMR 7057,*
Université Paris Diderot, SPC University,
10 Rue A. Domon et L. Duquet, F-75013 Paris, France

[2]*Laboratoire Sciences et Ingénierie de la Matière Molle,*
PSL Research University, ESPCI Paris, CNRS,
10 rue Vauquelin, F-75231 Paris cedex 05, France

[3]*Global Station for Soft Matter, Global Institution for Collaborative Research and Education, Hokkaido University, Sapporo, Japan*

(Dated: December 24, 2017)

* E-mail address: matthieu.roche@univ-paris-diderot.fr

MODELING OF THE STATICS AND THE DYNAMICS OF THE CONTACT LINE ON A SOFT SOLID

A. Theoretical model

The mechanical equilibrium in the bulk of the incompressible soft elastic layer is described by the Navier equations:

$$\vec{\nabla} \cdot \sigma = \vec{0} \text{ and } \vec{\nabla} \cdot \vec{u} = 0 \tag{1}$$

where $\vec{u}$ is the displacement field and σ is the stress tensor. This set of equations is completed by the condition of stress continuity at the boundary:

$$\sigma \cdot \vec{n} = \vec{t} + \gamma_s \vec{n}(\vec{\nabla} \cdot \vec{n}) \tag{2}$$

where $\vec{n}$ and $\vec{t}$ are the unit normal vector to the surface and traction forces exerted at the substrate boundary, respectively. γ_s is the surface tension of the solid. Note that we assume the surface tension of the gel to be the same for both the wetted and the dry parts of the gel. Hence there is no traction jump along the surface tangent of In addition, the soft elastic layer is bounded at the bottom , i.e at $y = -h_0$:

$$\vec{u}(x, -h_0) = \vec{0} \tag{3}$$

1. *Static problem*

Let us first consider the problem of a static force distribution $\vec{t} = (t_x(x), t_y(x))$ applied at the free boundary of a purely elastic solid with surface tension γ_S. Within this framework, the stress tensor σ is given, in component form, by the following constitutive relationship:

$$\sigma_{ij} = \mu_0 \left(\frac{\partial u_i}{\partial x_j} + \frac{\partial u_j}{\partial x_i} \right) - p\delta_{i,j} \tag{4}$$

where $\delta_{i,j}$ is the Kronecker delta symbol and p is the pressure field. This field is introduced as a Lagrange multiplier to enforce the incompressibility constraint.The equilibrium equations reduce to the Navier equations:

$$\vec{\nabla} \cdot \vec{u} = 0 \text{ and } \mu_0 \triangle \vec{u} - \vec{\nabla} p = 0 \tag{5}$$

In order for the linear elastic theory to be valid, the slope of the surface profile $u_y(x, y = 0) = \zeta(x)$ must be small everywhere, i.e $\zeta'(x) \ll 1$ where the prime denotes the derivative with respect

to x. Within this approximation, the boundary conditions (2)-(3) take the form:

$$\sigma_{yy} = 2\mu_0 \frac{\partial u_y}{\partial y} - p = t_y(x) + \gamma_S \frac{\mathrm{d}^2\zeta}{\mathrm{d}x^2} \tag{6}$$

$$\sigma_{xy} = \mu_0 \left(\frac{\partial u_y}{\partial x} + \frac{\partial u_x}{\partial y} \right) = t_x(x) \tag{7}$$

$$u_x(x, -h_0) = 0 \tag{8}$$

$$u_y(x, -h_0) = 0 \tag{9}$$

This problem can be solved by using a potential function φ for the displacement field defined as:

$$u_x = -\frac{\partial \varphi}{\partial y} \text{ and } u_y = \frac{\partial \varphi}{\partial x} \tag{10}$$

With this definition, the incompressiblity condition $\nabla \cdot \vec{u} = 0$ is automatically satisfied. Inserting the potential function into the Navier equations and rearranging the terms yields the biharmonic equation:

$$\triangle^2 \varphi = 0; \tag{11}$$

We now introduce the Fourier transform $\tilde{\varphi}$ of the potential function φ:

$$\varphi(x, y) = \frac{1}{2\pi} \int_{-\infty}^{\infty} \mathrm{d}k \tilde{\varphi}(k, y) e^{ikx} \tag{12}$$

Plugging this expression into the biharmonic equation yields a simple fourth-order linear differential equation for $\tilde{\varphi}(k, z)$:

$$\frac{\partial^4 \tilde{\varphi}}{\partial y^4} - 2k^2 \frac{\partial^2 \tilde{\varphi}}{\partial y^2} + k^4 \tilde{\varphi} = 0 \tag{13}$$

This equation has the following general solution:

$$\tilde{\varphi}(k, y) = Ae^{ky} + Be^{-ky} + Cye^{ky} + Dye^{-ky} \tag{14}$$

Now the four unknown constant A, B, C and D have to be determined using the boundary conditions (6)-(7)-(8)-(9). Written in terms of $\tilde{\varphi}(k, z)$, these BCs reads:

$$2\mu_0 ik \frac{\partial \tilde{\varphi}}{\partial y} - \frac{\mu_0 i}{k} \left(\frac{\partial^3 \tilde{\varphi}}{\partial y^3} - k^2 \frac{\partial \tilde{\varphi}}{\partial y} \right) = \tilde{t_y}(k) - \gamma_S ik^3 \tilde{\zeta} \quad \text{at } y = 0 \tag{15}$$

$$\mu_0 \left(-k^2 \tilde{\varphi} + \frac{\partial \tilde{\varphi}}{\partial x} \right) = \tilde{t_x}(k) \quad \text{at } y = 0 \tag{16}$$

$$\frac{\partial \tilde{\varphi}}{\partial y}|_{y=-h_0} = 0 \tag{17}$$

$$\tilde{\varphi}(x, -h_0) = 0 \tag{18}$$

This system of equation leads to the following expression for the Fourier transform $\tilde{\zeta}$ of the surface displacement field ζ:

$$\tilde{\zeta}(k) = \frac{\tilde{t_y}(k)(\sinh(2h_0k) - 2h_0k) - 2ih_0^2k^2\tilde{t_x}(k)}{k\left(2\left(h_0k^2(2h_0\mu_0 - \gamma_s) + \mu_0\right) + \gamma_s k\sinh(2h_0k) + 2\mu_0\cosh(2h_0k)\right)} \tag{19}$$

or in a more compact form:

$$\tilde{\zeta}(k) = \frac{1}{\gamma_s}\left[k^2 + \frac{\mu_0}{\gamma_s K(k)}\right]^{-1}\left(\tilde{t_y} - i\tilde{t_x}\frac{2h_0^2k^2}{\sinh(2h_0k) - 2h_0k}\right) \tag{20}$$

where:

$$K(k) = \left[\frac{\sinh(2h_0k) - 2h_0k}{2h_0^2k^2 + \cosh(2h_0k) + 1}\right]\frac{1}{2k} \tag{21}$$

In real space, the solution $\zeta(x)$ is thus given by:

$$\zeta(x) = \frac{1}{2\pi}\int_{-\infty}^{\infty} \mathrm{d}k\tilde{\zeta}(k)e^{ikx} \tag{22}$$

The single contact line

When the surface force is a line force, ie, when $t_x = f_x\delta(x)$ and $t_y = f_y\delta(x)$, then

$$\zeta(x) = \frac{f_y}{2\pi\gamma_s}\int_{-\infty}^{\infty}\mathrm{d}k\cos kx\left[k^2 + \frac{\mu_0}{\gamma_s K(k)}\right]^{-1} + \frac{f_x}{2\pi\gamma_s}\int_{-\infty}^{\infty}\mathrm{d}k\sin kx\left(\frac{2h_0^2k^2}{\sinh(2h_0k) - 2h_0k}\right)\left[k^2 + \frac{\mu_0}{\gamma_s K(k)}\right]^{-1} \tag{23}$$

Note that because of the finite thickness and the incompressibility constraint, the tangential f_x force also induces vertical displacements. When $h_0 \to \infty$, the second term of the right-hand side of the equation above vanishes and we recover the infinite depth result of Limat [1]:

$$\zeta_\infty(x) = \frac{f_y}{2\pi\mu_0}\int_{1/\Delta}^{\infty}\frac{\cos kx}{k + \frac{\gamma_S}{2\mu_0}k^2}\mathrm{d}k \tag{24}$$

where Δ is a macroscopic cut-off length due to the 2-D nature of the problem. Note that for an infinite depth, the vertical (tangent) force only produces a vertical (tangent) displacement.

The 2D rivulet

In the case of a 2D rivulet of width $2R$ similar to the one treated by Dervaux and Limat [2], the force distribution is given by $t_x = \gamma(\cos(\pi-\theta) - \cos(\pi-\theta_{eq}))\delta(x-R) + \gamma(\cos(\theta) - \cos(\theta_{eq}))\delta(x+R)$ and $t_y = \gamma\sin(\pi-\theta)\delta(x-R) + \gamma\sin(\theta)\delta(x+R) + \gamma\sin(\theta)/R * H(x+R)H(R-x)$, where H is the

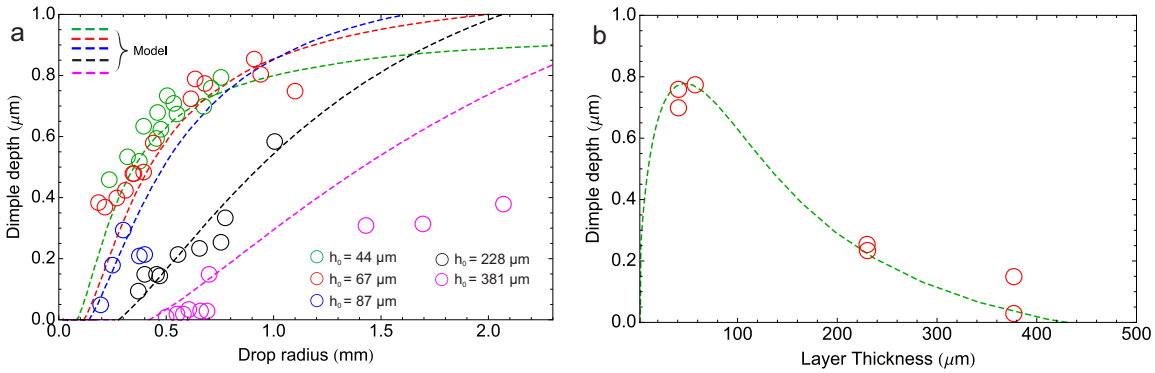

Figure 1. Prediction of the dimple depth as a function of (a) the droplet radius for various substrate thicknesses in the static case and (b) the thickness of the gel layer for a droplet with a contact radius of 1.3 mm.

Heaviside step function. The terms involving the difference between the cosines of the measured contact angle θ and the equilibrium contact angle θ_{eq} reflect the presence of hysteresis. For a set of experiments performed under identical conditions, the equilibrium contact angle is defined as the average of the measured contact angles. Even though the measured hysteresis is small, it has a significant effect on the depth of the dimple. Comparisons with experimental data in Fig. 2d of the main text and Fig. 1 below use this definition of the contact forces plugged into equation 23, and an effective radius of half the experimental radius in order to obtain the same Laplace pressure inside the drop, together with a surface tension of 40mN m^{-1}.

2. *Dynamic problem*

General solution for arbitrary rheology: We now consider the dynamical problem of a moving contact line on a soft solid, i.e the surface traction $\vec{t} = (t_x(x,t), t_y(x,t))$ now explicitly depends on time. In addition, and in stark contrast with the wetting problem on rigid substrate, dissipation now occurs mainly in the solid substrate. As documented by earlier studies, it is necessary to take into account the time-dependent response of the soft substrate in order to describe the motion of the contact line. In general linear viscoelastic materials, the stresses and strains are related through the linear relation:

$$\sigma(\vec{x},t) = \int_{-\infty}^{t} \mu(t-t')\frac{\partial}{\partial t'}\mathrm{d}t' - p(\vec{x},t)\mathbf{I} \tag{25}$$

with $\mathbf{I}$ the identity matrix. The Fourier transform with respect to time of Eq. 25 reads:

$$\hat{\sigma}(\vec{x},\omega) = \mu(\omega)\varepsilon(\vec{x},\omega) - \hat{p}(\vec{x},\omega)\mathbf{I} \tag{26}$$

with the particular definition of $\mu(\omega)$:

$$\mu(\omega) = i\omega \int_0^\infty \mu(t) \mathrm{e}^{-i\omega t} \mathrm{d}t \tag{27}$$

Using these definitions and Fourier-transforming equations (1), the moving contact line problem is described by the following equilibrium equation:

$$\vec{\nabla} \cdot \vec{\hat{u}} = 0 \text{ and } \mu(\omega) \triangle \vec{\hat{u}} - \vec{\nabla} \hat{p} = 0 \tag{28}$$

Under the time Fourier-transform, the boundary conditions (2)-(3) take the form:

$$\hat{\sigma}_{yy} = 2\mu(\omega) \frac{\partial \hat{u}_y}{\partial y} - \hat{p} = \hat{t}_y(\omega) + \gamma_S \frac{\mathrm{d}^2 \hat{\zeta}}{\mathrm{d}x^2} \tag{29}$$

$$\hat{\sigma}_{xy} = \mu(\omega) \left(\frac{\partial \hat{u}_y}{\partial x} + \frac{\partial \hat{u}_x}{\partial y} \right) = \hat{t}_x(\omega) \tag{30}$$

$$\hat{u}_x(x, -h_0) = 0 \tag{31}$$

$$\hat{u}_y(x, -h_0) = 0 \tag{32}$$

Note that equations (28)-(29)-(30)-(31)-(32), which describe the behavior of the time-Fourier-transforms of $\vec{\hat{u}}$ and $\hat{p}$, are strictly identical to the set of equation (1)-(6)-(7)-(8)-(9) of the static problem for $\vec{u}$ and p. The solution of the problem is therefore straightforward and reads:

$$\tilde{\hat{\zeta}}(k,t) = \frac{1}{\gamma_s} \left[k^2 + \frac{\mu(\omega)}{\gamma_s K(k)} \right]^{-1} \left(\tilde{\hat{t}}_y(k,\omega) - i\tilde{\hat{t}}_x(k,\omega) \frac{2h_0^2 k^2}{\sinh(2h_0 k) - 2h_0 k} \right) = \tilde{\hat{t}}_y(k,\omega) S(k,\omega) + \tilde{\hat{t}}_x(k,\omega) Q(k,\omega) \tag{33}$$

If we now focus on the case of a contact line moving at constant velocity, ie $t_x = \gamma(\cos\theta_{eq} - \cos\theta_{dyn})\delta(x - vt)$ and $t_y = \gamma \sin\theta \delta(x - vt)$, then the double Fourier-transform with respect to both time and space preserve the shape of the traction. In this case, we have simply: $\tilde{\hat{t}}_x(k,\omega) = \gamma(\cos\theta_{eq} - \cos\theta_{dyn})\delta(\omega + vk)$ and $\tilde{\hat{t}}_y(k,\omega) = \gamma \sin\theta \delta(\omega + vk)$ and thus:

$$\tilde{\hat{\zeta}}(k,\omega) = \gamma \sin\theta \delta(\omega + vk) S(k,\omega) + \gamma(\cos\theta_{eq} - \cos\theta_{dyn}) \delta(\omega + vk) Q(k,\omega) \tag{34}$$

The solution (33) can be inverted straightforwardly with respect to ω to give:

$$\tilde{\zeta}(k,t) = \mathrm{e}^{-ikvt} \frac{\gamma \sin\theta}{\gamma_s} \left[k^2 + \frac{\mu(-kv)}{\gamma_s K(k)} \right]^{-1} - i\mathrm{e}^{-ikvt} \frac{\gamma(\cos\theta_{eq} - \cos\theta_{dyn})}{\gamma_s} \left[k^2 + \frac{\mu(-kv)}{\gamma_s K(k)} \right]^{-1} \frac{2h_0^2 k^2}{\sinh(2h_0 k) - 2h_0 k} \tag{35}$$

The solution in real space is thus given by:

$$\zeta(x,t) = \frac{\gamma \sin\theta}{2\pi\gamma_s} \int_{-\infty}^{\infty} \mathrm{d}k \mathrm{e}^{ik(x-vt)} \left[k^2 + \frac{\mu(-kv)}{\gamma_s K(k)} \right]^{-1} \tag{36}$$

$$+ \frac{\gamma(\cos\theta_{eq} - \cos\theta_{dyn})}{2\pi\gamma_s} \int_{-\infty}^{\infty} \mathrm{d}k \mathrm{e}^{ik(x-vt)} \left[k^2 + \frac{\mu(-kv)}{\gamma_s K(k)} \right]^{-1} \frac{2h_0^2 k^2}{\sinh(2h_0 k) - 2h_0 k} \tag{37}$$

In the co-moving frame ($x' = x - vt$), the profile of the deformation $h(x')$ is independent of time:

$$h(x') = \frac{\gamma \sin\theta}{2\pi\gamma_s} \int_{-\infty}^{\infty} \mathrm{d}k e^{ikx'} \left[k^2 + \frac{\mu(-kv)}{\gamma_s K(k)} \right]^{-1} \tag{38}$$

$$+ \frac{\gamma(\cos\theta_{eq} - \cos\theta_{dyn})}{2\pi\gamma_s} \int_{-\infty}^{\infty} \mathrm{d}k e^{ikx'} \left[k^2 + \frac{\mu(-kv)}{\gamma_s K(k)} \right]^{-1} \frac{2h_0^2 k^2}{\sinh(2h_0 k) - 2h_0 k} \tag{39}$$

This expression is valid for arbitrary rheology at long time following the application of the line force and does not account for any transient regime that might occurs immediately following the application of the line force. In the formulation of the viscoelastic problem presented here, we are only focusing on the deformation induced by a single contact line because experimental results indicate that the dynamic contact angle does not depend on the droplet size. Because we are assuming that the surface tension of the gel is the same for both the wetted and the dry parts of the gel, we are therefore dealing with a pure traction boundary condition problem where the same (time-dependent) boundary condition is applied to the entire free boundary. In that case the correspondence principle applies [3] This principle would not apply if the Laplace pressure term was also included in the boundary condition or if different surface tensions act on the wetted and dry parts of the gels. In those cases, different boundary conditions would be applied to disjoint complementary sub-regions of the free boundary. Because these regions would change over time, the integral transform of the boundary conditions would not be obtainable and more work would be needed to solve this viscoelastic problem.

Selection of the dynamic contact angle: During dynamical wetting, the contact angle does not satisfy the Young's equation and there is a driving force at the contact line resulting from the imbalance of surface tension. This driving force is responsible for setting the contact line into motion. It is seen experimentally that there exists a relationship linking the dynamic contact angle and the velocity of the contact line. A huge amount of theoretical, numerical and experimental work has been devoted to the determination of this relation on rigid substrate. In general, the relation between dynamical contact angle and spreading velocity is found by balancing the dissipation in the liquid with the work done by the driving force at the contact line. In the case of wetting on soft substrate, the spreading velocity is orders of magnitude smaller than its rigid counterpart. This is due to the viscous dissipation in the solid substrate itself, as elastomer material usually possess very high viscous constants. We expand here an earlier result [4] for the case of a solid with surface

tension and for arbitrary velocities. The dissipation P_{film} in the substrate is given by:

$$P_{film} = \int_{\mathcal{B}} \mathrm{d}^2 x \sigma : \dot{\varepsilon} \tag{40}$$

where the integration is performed over the volume $\mathcal{B}$ of the substrate. Let us express the dissipation in terms of the time-Fourier-transform:

$$P_{film} = \frac{1}{4\pi^2} \int_{\mathcal{B}} \mathrm{d}^2 x \int_{-\infty}^{\infty} \mathrm{d}\omega \mathrm{d}\omega' (i\omega') \mathrm{e}^{i(\omega+\omega')t} \mu(\omega) \hat{u}_{ij}(\vec{x}, \omega) \hat{u}_{ij}(\vec{x}, \omega') \tag{41}$$

Following Long, Adjari, Leibler, we will assume that the four terms in the integral above contribute about equal quantities and we retain only the variation along the x-direction of the displacement in the z-direction. Dropping the factor $1/(4\pi^2)$, we get:

$$P_{film} \sim \int_{\mathcal{B}} \mathrm{d}^2 x \int_{-\infty}^{\infty} \mathrm{d}\omega \mathrm{d}\omega' (i\omega') \mathrm{e}^{i(\omega+\omega')t} \mu(\omega) \frac{\partial \hat{\zeta}}{\partial x}(\vec{x}, \omega) \frac{\partial \hat{\zeta}}{\partial x}(\vec{x}, \omega') \tag{42}$$

According to the Plancherel theorem, the previous integral can be rewritten as:

$$P_{film} \sim \int_{-h_0}^{0} \mathrm{d}z \int_{-\infty}^{\infty} \mathrm{d}\omega \mathrm{d}\omega' (i\omega') \mathrm{e}^{i(\omega+\omega')t} \mu(\omega) \int_{-\infty}^{\infty} k^2 \tilde{\hat{\zeta}}(k, \omega) \tilde{\hat{\zeta}}(-k, \omega) \mathrm{d}k \tag{43}$$

Using (34), the dual integral over the frequency domain is easily resolved. For the sake of simplicity we only retain terms in $\sin^2\theta$ in equation (34) and we get:

$$P_{film} \sim \int_{-h_0}^{0} \mathrm{d}z \int_{-\infty}^{\infty} (ikv) \mu(-kv) k^2 \gamma^2 \sin^2\theta S(k, -kv) S(-k, kv) \mathrm{d}k \tag{44}$$

Because the deformation penetrate to a depth of $|k|^{-1}$, the previous integral is further simplified as:

$$P_{film} \sim \gamma^2 v \sin^2\theta \int_{-\infty}^{\infty} (ik) \mu(-kv) k \mathrm{sign}(k) S(k, -kv) S(-k, kv) \mathrm{d}k \tag{45}$$

For a purely elastic material $\mu(\omega) = cste$ and the above integral is purely imaginary. We now use the Chasset-Thirion model defined by:

$$\mu(\omega) = \mu_0 (1 + (i\omega\tau)^m) \tag{46}$$

Inserting this definition in (45), we get:

$$P_{film} \sim \mu_0 \gamma^2 v \sin^2\theta |v\tau|^m \int_0^{\infty} |k|^{m+2} S(k, -kv) S(-k, kv) \mathrm{d}k \tag{47}$$

or:

$$P_{film} \sim \left(\frac{\gamma \sin\theta}{\gamma_s}\right)^2 v\mu_0 |v\tau|^m \int_0^{\infty} \frac{|k|^{m+2}}{\left(k^2 + \frac{\mu(-kv)}{\gamma_s K(k)}\right)\left(k^2 + \frac{\mu(kv)}{\gamma_s K(-k)}\right)} \mathrm{d}k \tag{48}$$

The dissipated power P_{film} is equal to the work $v\gamma(\cos\theta - \cos\theta_{eq})$ of the driving force to yield:

$$\frac{(\cos\theta - \cos\theta_{eq})}{\sin^2\theta} \sim \left(\frac{\gamma}{\gamma_s}\right)\frac{\mu_0}{\gamma_s}|v\tau|^m \int_0^\infty \frac{|k|^{m+2}}{\left(k^2 + \frac{\mu(-kv)}{\gamma_s K(k)}\right)\left(k^2 + \frac{\mu(kv)}{\gamma_s K(-k)}\right)}\mathrm{d}k \tag{49}$$

As shown in Fig. 3a and Fig. 3b in the paper, the relation (49) provides a very accurate description of the experimental data, for all velocities and thickness values. Furthermore, the quantity $\frac{(\cos\theta - \cos\theta_{eq})}{\sin^2\theta}$ is indeed proportional to v^m, for the full range of velocity investigated experimentally. This demonstrates that the previous expression can be approximated by the following somewhat simpler low velocity expression:

$$\frac{(\cos\theta - \cos\theta_{eq})}{\sin^2\theta} \sim \left(\frac{\gamma}{\gamma_s}\right)\frac{\mu_0}{\gamma_s}|v\tau|^m \int_0^\infty \frac{|k|^{m+2}}{\left(k^2 + \frac{\mu_0}{\gamma_s K(k)}\right)^2}\mathrm{d}k \tag{50}$$

B. "Neumann-like" force balance at the triple line cannot explain the experimental data

We now present another theory to describe the selection of the contact angle, introduced in [5]. The hypothesis behind the model is that the Neumann construction that is valid at equilibrium still holds in the dynamical case. Because the ridge rotates during its propagation by an angle $\varphi = \theta - \theta_{eq}$, the apparent contact angle should also rotate to accommodate the rotation of the ridge. According to [5], the rotation of the ridge φ is given by the symmetric part of the surface deformation profile in the co-moving frame, i.e:

$$\tan\varphi = \lim_{x\to 0}\frac{1}{2}(h'(x) - h'(-x)) \tag{51}$$

$$= \frac{\gamma\sin\theta}{2\pi\gamma_s}\int_{-\infty}^{\infty}\Re\left[\frac{-ik}{k^2 + \frac{\mu(-kv)}{\gamma_s K(k)}}\right]\mathrm{d}k \tag{52}$$

As in the dissipated power model, for a purely elastic material $\mu(\omega) = cste$, the above integral is purely imaginary. At low enough velocities, the above expression reduces to:

$$\frac{\tan(\theta - \theta_{eq})}{\sin\theta} = \left(\frac{\gamma}{\pi\gamma_s}\right)\frac{\mu_0}{\gamma_s}|v\tau|^m \int_0^\infty \frac{|k|^{m+1}}{K(k)\left(k^2 + \frac{\mu_0}{\gamma_s K(k)}\right)^2}\mathrm{d}k \tag{53}$$

We can now check the validity of model (52). First it should be noted that, up to a multiplicative factor, the model (53) converge to the dissipation model (49) in the limits where $\varphi, V \ll 1$ and $h_0 \to \infty$ (since $\lim_{h_0\to\infty} K(k) = 1/(2k)$). In that case, we have:

$$\theta - \theta_{eq} = \left(\frac{\gamma\sin\theta_{eq}}{\gamma_s}\right)\frac{n2^n}{\sin(n\pi)}\left(\frac{v\tau\mu_0}{\gamma_s}\right)^m \tag{54}$$

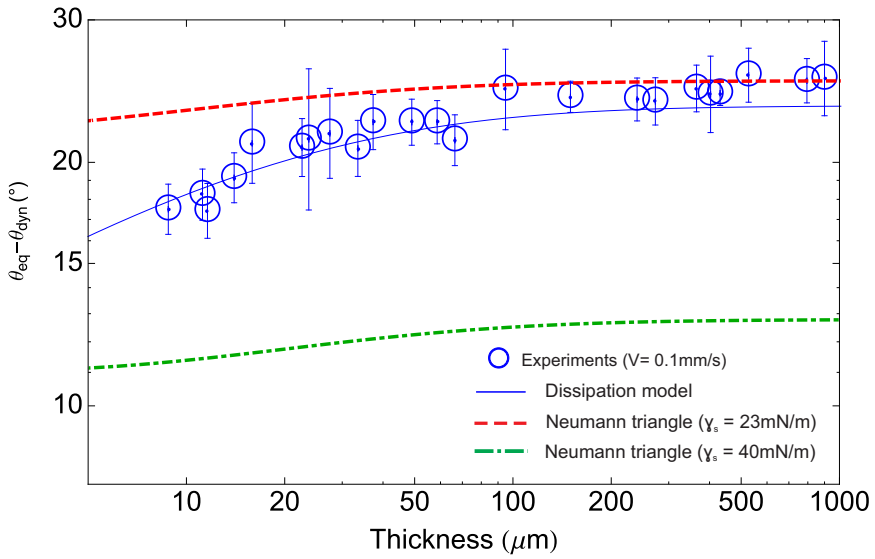

Figure 2. "Neumann-like" force balance at the triple line cannot explain the experimental data. Comparison between the dissipation model (equation (49)) and the Neumann construction (equation (53)). Using the value for $\gamma_s = 40$mN/m obtained from the static profiles yields a very poor fit to the experimental data (green dot-dashed line). Letting γ_s be a free parameter, the best fit was obtained for $\gamma_s = 23$mN/m. As mentioned above, this reproduces rather well the experimental data at large thickness but fail to capture the data at small h_0.

So we expect that at large thickness, this model should provide an accurate description of the experimental data (up to a multiplicative constant). As can be seen on Fig. 2, the Neumann triangle indeed yields a very poor fit to the experimental data (green dot-dashed line) using the value for $\gamma_s = 40$mN/m obtained from the static profiles. Letting γ_s be a free parameter (the best fit was obtained for $\gamma_s = 23$mN/m), this model however reproduces rather well the experimental data at large thickness but fail to capture the data at small h_0.

C. Independence of the static contact angle on the elasticity of the substrate

A careful examination of the asymptotics of the vertical displacement $\zeta(x)$ with respect to the wavenumber k of the displacement in the static case sheds some light on the physical explanation of the reason why the static contact angle is independent of the elasticity of the substrate.

Our analysis is inspired by the one followed by Style and Dufresne in their 2012 paper [6]. We consider the large droplet limit where the contact angle is independent of the droplet size. The

vertical displacement is given by Eq. 20:

$$\tilde{\zeta}(k) = \frac{1}{\gamma_s}\left[k^2 + \frac{\mu_0}{\gamma_s K(k)}\right]^{-1}\left(\tilde{t_y} - i\tilde{t_x}\frac{2h_0^2k^2}{\sinh(2h_0k) - 2h_0k}\right) \tag{55}$$

where:

$$K(k) = \left[\frac{\sinh(2h_0k) - 2h_0k}{2h_0^2k^2 + \cosh(2h_0k) + 1}\right]\frac{1}{2k} \tag{56}$$

The interesting part of this expression is the amplitude term:

$$\begin{aligned} A(h_0, k) &= \frac{1}{\gamma_s}\left[k^2 + \frac{\mu_0}{\gamma_s K(k)}\right]^{-1} \\ &= \left[\gamma_s k^2(1 + \frac{\mu_0}{\gamma_s k^2 K(k)})\right]^{-1} \end{aligned} \tag{57}$$

as it contains all of the information on the physics of the problem and, specifically, on the contributions of the properties of the gel, such as its interfacial tension γ_s and its shear modulus μ_0, to the damping of the displacement.

We shall then focus on the asymptotic of $A(h_0, k)$ for large wavenumbers k, *i.e.* short wavelengths. In this limit, the elastic term $\mu_0(\gamma_s k^2 K(k))^{-1}$ vanishes for all values of h_0: perturbation damping is controlled by surface tension at large wavenumbers. We can also show that elasticity is the main contributor to the damping at small wavenumbers, *i.e.* large wavelengths.

From what we have just established, it is clear that the amplitude of displacements in the vicinity of the contact line is set by the ratio of the traction force to the surface tension of the solid, with no contribution of elasticity. A direct consequence of this is that strains, and hence slopes and angles, close to the contact line are also independent of the elastic response of the bulk. As the latter is dependent on the thickness of the sample, we conclude that thickness does not play a role in setting the static contact angle.

Thickness affects in fact the cross-over wavelength between the long-wavelength and the short-wavelength responses. When the sample is thick, $A(h_0, k)$ involves a characteristic length that is the elastocapillary length $\ell_s = \gamma_s/\mu_0$ while this length scale becomes $\ell_t = (\gamma_s h_0^3 \mu_0^{-1})^{1/4}$ in the thin-coating limit. These two lengths set the crossover between the two wavelength regimes depending on the thickness of the sample. Note that this crossover had already been identified by Style and Dufresne[6] although they did not provide an expression for ℓ_t. These length-scales do not affect the dependence of the contact angles on the thickness of the sample that we established at the previous paragraph.

D. Testing the importance of 3D effects

Our model is bidimensional and neglects effects due to the size of the droplets in the dynamic case. We have made this assumption as measurements of the relation between the dynamic contact angle and the velocity of the receding contact line for droplets of different sizes showed no dependence on the latter (Fig. 3).

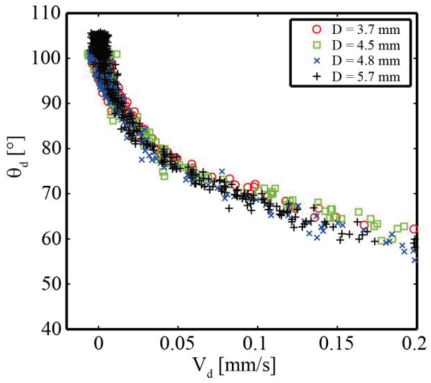

Figure 3. Test of the dependence of the relation between the dynamic contact angle and the velocity at which the contact line recedes on the size of the droplet.

---

[1] L. Limat, EPJ E **35**, 134 (2012).

[2] J. Dervaux and L. Limat, Proc. R. Soc. A **471**, 20140813 (2015).

[3] G. A. C. Graham, Q. Appl. Math. **26**, 167 (1968).

[4] D. Long, A. Ajdari, and L. Leibler, Langmuir **12**, 5221 (1996).

[5] S. Karpitschka, S. Das, M. van Gorcum, H. Perrin, B. Andreotti, and J. H. Snoeijer, Nat. Commun. **6**, 7891 (2015).

[6] R. W. Style and E. R. Dufresne, Soft Matter **8**, 7177 (2012).